analytical chemistry

ARTICLE

pubs.acs.org/ac

Analysis of Counterfeit Pharmaceutical Tablet Cores Utilizing Macroscopic Infrared Spectroscopy and Infrared Spectroscopic Imaging

Adam Lanzarotta,*[,†] Kendra Lakes,[‡] Curtis A. Marcott,[§] Mark R. Witkowski,[†] and Andre J. Sommer[‡]

[†]Trace Examination Section, FDA Forensic Chemistry Center, 6751 Steger Drive, Cincinnati, Ohio 45237, United States

[‡]Molecular Microspectroscopy Laboratory, Department of Chemistry and Biochemistry, Miami University, Oxford, OH 45056, United States

[§]Light Light Solutions, Athens, Georgia 30608, United States

ABSTRACT: Advantages and limitations of analyzing authentic and counterfeit pharmaceutical tablets with both macro (nonimaging) attenuated total internal reflection Fourier transform infrared (ATR-FT-IR) spectroscopy and micro ATR-FT-IR spectroscopic imaging have been evaluated. The results of this study demonstrated that micro ATR imaging was more effective for extracting formulation information (sourcing), whereas a macro ATR approach was better suited for counterfeit detection (screening). More importantly, this study demonstrated that a thorough analysis of the counterfeit core can be achieved by combining the results of both techniques.

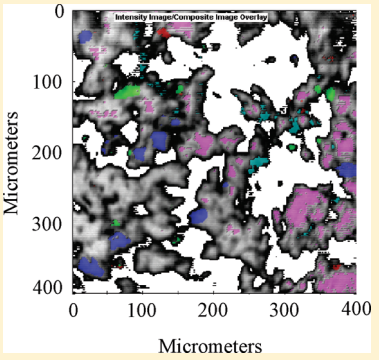

Counterfeit pharmaceutical products pose a serious public health risk and expose the unknowing consumer to numerous potential health hazards. Counterfeit pharmaceutical dosages may contain harmful impurities, may be ineffective, and/or may have altered bioavailability.[1] An additional consequence of counterfeit products is the adverse economic impact suffered by the legitimate pharmaceutical manufacturer. The United States Food and Drug Administration's (FDA) Forensic Chemistry Center (FCC) has been involved in the analysis of counterfeit products since the early 1990s. Initial analyses by the FCC focused on active pharmaceutical ingredients (APIs) and have evolved to include counterfeit dosage forms, packaging materials, medical devices, and over-the-counter (OTC) products.

The FCC utilizes a multidisciplinary approach to determine if the suspect product is consistent with the authentic product (counterfeit detection) and to determine if two or more suspect products share a common origin (counterfeit sourcing). The techniques typically employed are listed in Table 1 and are separated into three distinct groups. Each group provides unique information about a counterfeit product. Physical analysis (group 1) includes techniques that are employed to collect basic physical information on a sample such as visual images, weights, dimensions, and color. These methods are useful as a rapid screen and tend to detect less sophisticated, poor quality counterfeit products. Samples whose physical characteristics are closer to the authentic products require chemical analyses (groups 2 and 3). Group 2 includes chromatographic and mass spectrometric techniques; the primary functions of which are to identify/quantify APIs and detect product impurities. As the sophistication of counterfeit products increases, it becomes more difficult to establish authenticity just by testing the suspect product for the absence/presence or concentration of the API. Instead, a more comprehensive analysis is needed that involves examination of the entire product, which includes, but is not limited to, the tablet coating, core, capsule shell, capsule contents, and the packaging components.

Group 3 techniques provide elemental and molecular information. Vibrational spectroscopic techniques are commonly employed because they allow solid state analysis, which provides the ability to examine tablet coatings, cores, packaging, etc. with limited sample preparation.[2−7] Further, these techniques can often differentiate API polymorphs (different API crystalline forms).[8,9] This capability is important since the crystalline form of an API can affect its efficacy, stability, and solubility, which can have a significant impact on the toxicity of the drug and/or the bioavailability of the drug in the body.[10−14] As a consequence, having the proper crystalline form of the API can be just as important as having the correct API.[15] Since excipients also directly affect drug release efficacy, API stability,[16−19] and tablet pH,[20] similar health hazards can be associated with having an improper excipient profile. The presence of the incorrect excipients and/or absence of correct excipients can create API

Received: April 15, 2011
Accepted: June 7, 2011
Published: June 07, 2011

Table 1. Techniques Used by the Forensic Chemistry Center for the Analysis of Counterfeit Pharmaceuticals

physical analysis, toolmarks	chemical, assay, impurities	formulation
Physical Properties	Chromatographic and Mass Spectrometric Techniques	Vibrational Spectroscopy
weights	HPLC	FT-IR
measures	gas chromatography	Raman
hardness testing	ion chromatography	NIR
color	headspace GC/MS	
photo documentation	capillary electrophoresis	Elemental
stereoscopic light microscopy	thin layer chromatography	SEM-EDX
polarized light microscopy	GC/MS	AA
scanning electron microscopy	LC−MS	ICP-MS
image analysis	DART-FT-MS	
long-wavelength UV		
comparative microscope		

stability issues, which can lead to faster API degradation, higher impurity levels, and ultimately a greater potential for adverse patient reactions.[21−24] Because vibrational spectroscopic techniques are selective and sensitive to most APIs, excipients, and subtle API crystallinity differences, the role of these techniques is continuing to expand for the analysis of counterfeit pharmaceutical products.[2,4−7]

Near infrared (NIR) imaging is one such technique that has been employed for the analysis of counterfeit pharmaceutical tablets.[25−27] However, the use of this technique has been limited because it involves examining broad overtone and combination bands, which can make it difficult to identify APIs and excipients in complex tablet matrixes. Another vibrational technique that has been more selective for APIs, Raman spectroscopy, has also been employed in several pharmaceutical analyses[28−34] as well as in forensic investigations.[2,4−6,35] In some cases Raman mapping has been used to determine the formulations of cross-sectioned tablets.[4,6] However, Raman mapping has traditionally been limited to small sample areas to reduce long data acquisition times. Further, because of their molecular structure, pharmaceutical excipients are either Raman inactive or weak Raman scatterers. On the other hand, FT-IR spectroscopy is much more sensitive to excipients, which is why this technique is often used in conjunction with Raman spectroscopy for studies that require comprehensive vibrational spectroscopic characterization of both excipients and APIs.

Like Raman mapping, micro ATR imaging is a well-established approach that has been employed for a wide range of pharmaceutical applications.[35−41] There are several specific benefits associated with this approach in addition to the benefits shared by all vibrational spectroscopic techniques. These include controlled path length, which is independent of the sample thickness (assuming the depth of penetration is smaller than the sample thickness) and much faster acquisition times (minutes vs hours) for large image areas compared to Raman mapping experiments. Several studies have employed micro ATR imaging for the analysis of counterfeit pharmaceutical tablets.[35,41] Although each of these studies successfully differentiated suspect and authentic tablet formulations prior to this work, an exhaustive study was not conducted (i.e., sampling statistics, comparison of the imaging methods to more established methods, etc.). As a result, the focus of the current study was to evaluate the advantages and limitations of using micro ATR imaging for the analysis of counterfeit pharmaceutical tablets. Phase I involved a comparison of the theoretical sampling statistics of macro ATR and micro ATR imaging. Phases II and III evaluated experimental capabilities of each individual technique for characterizing and detecting counterfeit tablets, respectively. Phase IV evaluated the capabilities of the micro ATR imaging and macro ATR approaches when used in tandem.

EXPERIMENTAL SECTION

Materials. The three authentic pharmaceutical products were obtained directly from the manufacturers and have known API/excipient formulations. The six counterfeit tablets were taken from adjudicated criminal cases. The suspect tablets were chosen because they are three of the most commonly counterfeited prescription pharmaceuticals and because they contain sophisticated core formulations (i.e., the correct API and one or more excipients known to be present in the authentic formulation). It should be noted that the tablet coating provides additional information when examining or sourcing counterfeit tablets. However, the focus of this manuscript will be exclusively on the tablet cores.

Sample Preparation: Macro ATR. After removal of the coating (if present), roughly one-fourth of each authentic and suspect tablet was ground with a mortar and pestle. A small amount (∼10 mg) of the ground composite was placed directly onto the internal reflection element (IRE). The pressure arm was then lowered to provide the amount of force recommended by the manufacturer. Each ground tablet composite was analyzed in duplicate.

Sample Preparation: Micro ATR Imaging. Roughly one-half of each authentic and suspect tablet was embedded and cross-sectioned prior to analysis using a similar process described by Lanzarotta et al.[42] Instead of using a thermoplastic adhesive, the current study employed an epoxy stabilizing medium. Each tablet was analyzed in triplicate.

Instrumentation. Macro ATR spectra were acquired on a Thermo Nicolet 8700 main bench FT-IR spectrometer equipped with a Durascope ATR accessory (Smith's Detection), which contains a diamond coated ZnSe IRE (64 coadditions, 4 cm^{-1} resolution). Micro ATR images were collected on a Perkin-Elmer Spotlight 300 FT-IR imaging system (400 μm × 400 μm image, 1 scan per pixel, 1.56 μm × 1.56 μm pixel resolution and 16 cm^{-1} spectral resolution). Spectra from these images were compared to pure compound/reference standard spectra that were collected on a Perkin-Elmer Spectrum 100 main bench FT-IR

dx.doi.org/10.1021/ac200957d |Anal. Chem. 2011, 83, 5972–5978

spectrometer outfitted with a Universal Diamond/KRS-5 ATR accessory (32 coadditions, 16 cm^{-1} resolution). Spectral resolution of the macro ATR study was not the same as the ATR imaging study to keep image collection times to a minimum (13.3 min per image). The images were analyzed using Spectrum Image-Spotlight software, version 400 R1.6.4.0394 (Perkin-Elmer) and ISys software, version 5.0 (Malvern Instruments).

RESULTS AND DISCUSSION

Theoretical Sampling Considerations. Theoretical sampling was determined for micro ATR imaging by evaluating the sampled-mass to tablet-mass ratio, which was calculated by first considering the volume of sample analyzed by each pixel. Each spatial element had lateral dimensions of 1.56 μm × 1.56 μm. The depth, d_p, was calculated using eq 1:

$$d_p = \frac{\lambda}{2\pi n_c \left[\sin^2\theta - \left(\frac{n_s}{n_c}\right)^2\right]^{1/2}} \quad (1)$$

where λ is the wavelength of light, n_c is the refractive index of the IRE, n_s is the refractive index of the sample, and θ is the incident angle of the radiation.[43] Although the sampling depth can be as large as $3d_p$, d_p was employed to compare both techniques.[44] Since micro ATR imaging was conducted using an off-axis approach, the depth of penetration changes slightly from point-to-point.[45−47] However, for this study, the values calculated using eq 1 are assumed to approximate the average depth of penetration.

The sampling volume can be approximated as a triangular prism whose base is the lateral dimension (1.56 μm × 1.56 μm) and height is d_p using eq 2.

$$V = \frac{1}{2}\text{Area}_{\text{Pixel}} d_p \quad (2)$$

The mass of sample detected per pixel was determined by considering the volume calculated from eq 2 and the density of the material. Since tablets are multicomponent samples, the density of microcrystalline cellulose (d = 304 kg/m^3), a common major component by weight, was used for this estimation. At a wavelength of 6 μm (1666 cm^{-1}), a sample mass of 0.37 pg was detected by each pixel. The mass of sample interrogated by each 400 μm × 400 μm image was therefore 2.5 × 10^{-5} mg (25 ng). When considering a tablet mass of 630 mg for tablet A, the theoretical sampled-mass to tablet-mass ratio using this technique was only 3.9 × 10^{-8} or 39 ppb. The sampled-mass to tablet-mass ratios for each authentic tablet have been provided in Table 2 for both the micro ATR imaging technique and the macro ATR technique. Since the infrared active area of the macro ATR accessory is circular (r = 500 μm), the sample volume was estimated as a cone whose volume could be calculated using eq 3.

$$V = \frac{1}{3}\pi r^2 d_p \quad (3)$$

A sampled-mass to tablet-mass ratio of 180 ppb was calculated for authentic tablet A, which was approximately 4.5 times the ratio achieved with the micro imaging method.

To a first approximation, these sampling volumes appear unrepresentative compared to the total tablet volumes. However, both techniques may actually offer representative sampling if certain conditions are met. The macro technique may be representative if the fraction of the tablet exposed to the IRE is taken from a ground composite (assuming the sampling area is much greater than the individual particle sizes within the ground sample). The micro ATR imaging technique may offer representative sampling if the tablets are well-blended. However, since the manufacturing processes of counterfeit tablets are unknown, this assumption can not often be made, which is why several replicates of the same tablet should be analyzed when using this technique. One could argue that more representative sampling may be achieved for the micro ATR imaging approach by grinding the tablet into a composite. However, this would limit the spectral purity advantage of this method.[40,48]

Table 2. Sampled-Mass to Tablet-Mass Ratio Was Calculated for Both the Macro ATR and the Micro ATR Imaging Techniques Detailed in This Study[a]

		fraction of tablet interrogated	
tablet set	tablet mass (mg)	ATR imaging (ppb)	macro ATR (ppb)
A	630	39	180
B	360	68	310
C	620	40	180

[a] Values assume $n_{\text{microcrystalline cellulose}}$ = 1.55, n_{Ge} = 4.0, n_{diamond} = 2.4, incident angle imaging = 27°, incident angle macro = 45°, λ = 6 μm.

Expected Results: Counterfeit Detection vs Counterfeit Characterization. The macro ATR technique interrogates larger sample masses, necessitates minimal sample preparation, and requires collection times on the order of minutes. Consequently, a suspect spectrum can typically be generated and compared to a stored (library) authentic spectrum quickly. Therefore, the macro ATR technique is expected to be more effective for counterfeit detection.

Although the micro ATR imaging technique interrogates smaller sample masses, this technique examines localized components that are larger than the detector pixels, which provides spectra that are often characteristic of nearly pure compounds (increases confidence of analyte identification). For macro ATR the individual particle sizes are relatively small compared to the sampling area. Since most tablet formulations are multicomponent mixtures, the result is a complex mixture spectrum, which is why this technique usually requires spectral subtraction for characterization. The subtraction approach can only be effective until subtraction residuals dominate the spectrum. At this point a direct comparison to a standard becomes difficult. The advantage for characterizing tablet formulations is therefore expected to go to the micro ATR imaging technique.

Counterfeit Characterization. *Micro ATR Imaging.* The second phase of this study compared the macro ATR and micro ATR imaging techniques' ability to characterize counterfeit tablet formulations. A representative ATR image from authentic tablet A has been provided in Figure 1. The gray regions of the image correspond to component mixtures and the white regions correspond to areas of poor contact, which are due to either porosity of the tablet or ineffective cross-sectioning of the microtome procedure. The following five components were detected in the image: API-A (cyan), calcium phosphate dibasic (green), microcrystalline cellulose (magenta), carboxymethyl cellulose (blue), and an inorganic stearate (red). Component spectra from authentic tablet A have been provided in Figure 2 along with the corresponding standard spectra. The agreement

between spectra of the API and those of the standard, microcrystalline cellulose, calcium phosphate dibasic, and carboxymethyl cellulose sodium salt are representative of most components detected using the imaging technique. However, the inorganic stearate was one example of an excipient whose spectrum contained absorptions characteristic of another material. Because of their small particle size and use as lubricants, inorganic stearates often coat the API and other excipient particles in the blending process,[49] which is why most bands in the fingerprint region were attributed to API-A. Despite these additional absorptions, the general bands of an inorganic stearate could still be identified (indicated with arrows in Figure 2). The positions of the antisymmetric and symmetric stretch of the carboxylate anion are located at 1570 and 1455 cm^{-1}, respectively.[50] The CH_2 stretching absorptions near 2900 cm^{-1}, although not specific alone, provide structural information when compared with the carboxylate bands.

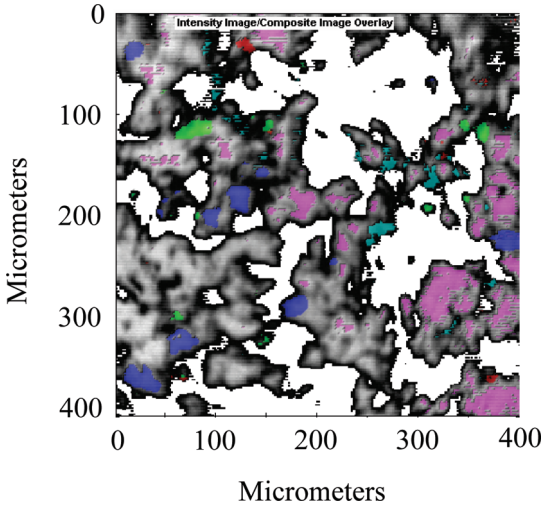

Figure 1. Representative image for authentic tablet A. API-A (cyan), calcium phosphate dibasic (green), microcrystalline cellulose (magenta), carboxymethyl cellulose sodium salt (blue), and an inorganic stearate (red) were detected. Gray and white regions correspond to component mixtures and areas of poor contact, respectively.

The imaging data for each authentic and suspect tablet have been listed in Table 3. As few as three components (suspect tablet B-1) and as many as six components (suspect tablets C-1 and C-2) were detected. An average of 4.7 and 4.8 components per tablet were detected for the authentic and suspect tablets, respectively. Considering that the sampling masses were only in the part per billion range, these data demonstrate that both the authentic and counterfeit tablets were relatively well blended.

Macro ATR. Table 3 includes the components that were detected in each authentic and suspect formulation using the macro approach. As few as two components (authentic tablet B) and as many as five components (suspect tablets A-2, C-1 and C-2) were detected using a spectral subtraction process. Spectral subtraction is a sequential process involving the subtraction of standard spectra from a tablet spectrum and subsequent resultant spectra. For example, the spectrum corresponding to authentic tablet A, illustrated in Figure 3, was searched ($search_1$) using a user-created ATR library. The ATR library contained over 600 individual standard spectra. The top match for $search_1$ was the labeled API (API-A). The API-A standard spectrum was then subtracted from the authentic tablet A spectrum. When the resultant spectrum (S_1) was searched ($search_2$), several stearates were listed as top matches. The inorganic stearate spectrum was then subtracted from S_1, yielding resultant spectrum S_2. The subtraction, search, and interpretation process was performed four times. $Search_5$ did not return any additional information. In

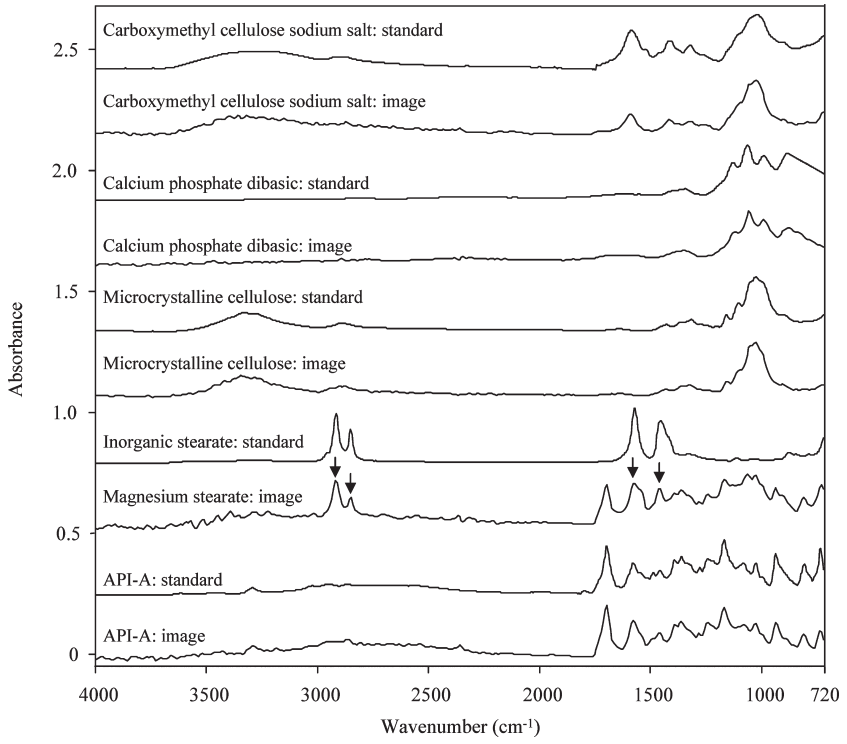

Figure 2. Micro ATR-FT-IR (germanium IRE) imaging spectra of each component detected in authentic tablet A along with standard spectra collected on an ATR-FT-IR main bench (diamond IRE) spectrometer.

dx.doi.org/10.1021/ac200957d |*Anal. Chem.* 2011, 83, 5972–5978

Table 3. Tablet Characterization[a]

	authentic A		suspect A1		suspect A2		authentic B		suspect B1		suspect B2		authentic C		suspect C1		suspect C2	
	micro	macro	micro	macro	micro	macro	micro	macro	micro	macro	micro	macro	micro	macro	micro	macro	micro	macro
API-A	X	X	X	X	X	X	–	–	–	–	–	–	–	–	–	–	–	–
API-B	–	–	–	–	–	–	X	X	X	X	X	X	–	–	–	–	–	–
API-C	–	–	–	–	–	–	–	–	–	–	–	–	X	X	X	X	X	X
MCC	X	X	X	X	X	X	X	–	X	X	X	X	X	X	X	X	X	X
CPD	X	X	–	–	–	–	–	–	–	–	–	–	–	–	–	–	–	–
CMC	X	–	–	–	–	–	X	–	–	–	–	–	X	–	–	–	–	–
SUC	–	–	X	X	–	–	–	–	–	–	–	–	–	–	–	–	–	–
ALM	–	–	–	–	X	X	X	X	–	–	X	X	X	X	–	–	–	–
CHP	–	–	X	–	X	X	–	–	–	–	–	–	–	–	–	–	–	–
TLC	–	–	–	–	X	X	–	–	–	–	–	–	–	–	X	X	X	X
STR	–	–	–	–	–	–	–	–	X	X	–	–	–	–	X	X	X	X
INS	X	X	X	–	–	–	–	–	–	–	X	X	–	–	X	–	X	–
INC	–	–	–	–	–	–	–	–	–	–	–	–	X	X	X	X	X	X

[a] Acronyms: microcrystalline cellulose (MCC), calcium phosphate dibasic (CPD), carboxymethylcellulose sodium salt (CMC), sucrose (SUC), α lactose monohydrate (ALM), calcium hydrogen phosphate dihydrate (CHP), talc (TLC), starch (STR), inorganic stearate (INS), and inorganic carbonate (INC).

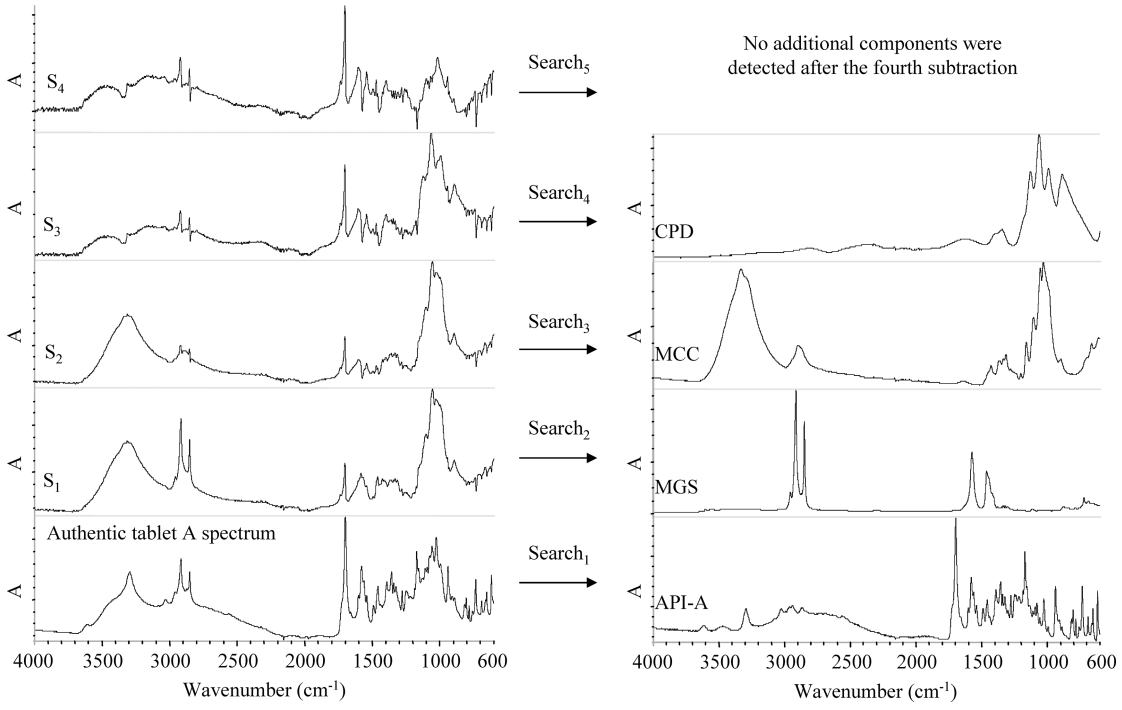

Figure 3. Subtraction process used in the current investigation.

most cases, the library searches yielded no additional components after a fourth iteration. This was due, in part, to the presence of spectral subtraction residuals.

Comparison. The micro ATR imaging technique detected at least as many components as the macro ATR method for each tablet and in every case but three (suspect tablets A-2, B-1, and B-2), additional components were detected using this approach. Overall, an average of 3.9 and 4.8 components per tablet were detected using the macro ATR and micro ATR imaging methods, which confirms that the micro ATR imaging approach was more effective for characterizing tablet formulations.

Counterfeit Detection. *Micro ATR Imaging.* The only means to establish authenticity by using the imaging approach was to determine qualitative formulation differences between the suspect and authentic tablets. For example, it was concluded that suspect tablet B-1 was counterfeit because it contained starch, a component not present in the known authentic formulation (Table 3). By this same line of reasoning, one might conclude that suspect tablet B-2 is counterfeit since it contained an ingredient not detected in any of the three authentic tablet B images (an inorganic stearate). However, the authentic tablet B formulation contains an inorganic stearate, albeit at a small concentration, which was probably why it was not detected. One may be inclined

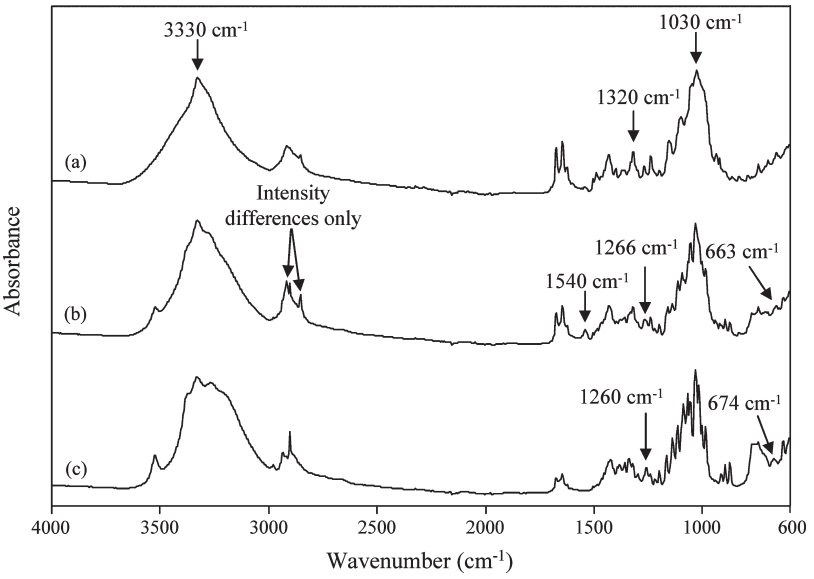

Figure 4. Representative macro ATR spectra of suspect tablet B-1 (a), suspect tablet B-2 (b), and authentic table B (c). The arrows indicate inconsistencies between the suspect tablets and authentic tablet B.

to conclude that suspect tablet B-2 is counterfeit because one component detected in authentic tablet B (carboxymethylcellulose sodium salt) was not detected in any of the three suspect tablet B-2 images (Table 3). However, the inability to detect a component, such as this negative finding, does not positively indicate a difference.[51] On the basis of these results, the authenticity of suspect tablet B-2 would be inconclusive.

Macro ATR. Macro ATR spectra for the authentic and two suspect samples from tablet set B can be viewed in Figure 4. The authentic tablet core was easily differentiated from both suspect tablet cores based on a one-to-one comparison of the infrared absorption bands (differences have been indicated with arrows in Figure 4). Differences between the authentic tablet and suspect tablet B-1 can be seen in the fingerprint region (around 1000 cm^{-1}) and in the region between 3700 and 2500 cm^{-1}. More subtle differences can be observed between the authentic tablet B and suspect tablet B-2 spectra. Band intensity differences were observed around 2900 cm^{-1}, and qualitative differences were observed in the fingerprint region. The suspect tablet B-2 spectrum contained a relatively small peak at 1540 cm^{-1} that was not present in the authentic tablet B spectrum. The wavenumber positions of several peaks in the suspect tablet B-2 spectrum are shifted relative to the authentic tablet B spectrum (from 1260 cm^{-1} in the authentic spectrum to 1266 cm^{-1} in the suspect spectrum and from 674 to 663 cm^{-1}, respectively). On the basis of these differences, it was concluded that the macro ATR spectra from suspect tablets B-1 and B-2 were not consistent with the authentic tablet B macro ATR spectrum.

Comparison of Micro ATR Imaging to Macro ATR. In five out of the six cases, both techniques were able to determine the authenticity of a suspect tablet; suspect tablets A-1, A-2, B-1, C-1, and C-2 were counterfeit. However, the micro ATR imaging and macro ATR results generated from suspect tablet B-2 is a working example of why the macro ATR method is better suited for counterfeit detection. While the macro ATR technique only needed slight spectral differences to distinguish a counterfeit and authentic tablet, the micro ATR imaging often needs to detect a component not present in the authentic formulation to provide a conclusive determination of authenticity.

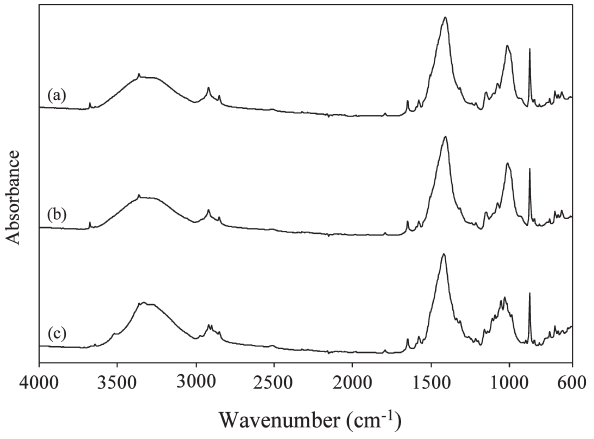

Figure 5. Representative macro ATR spectra of suspect tablet C-1 (a), suspect tablet C-2 (b) and authentic tablet C (c).

Benefits of Using Both Techniques Comprehensively. The fourth and final phase of this study investigated the advantages of using both techniques comprehensively. For example, using the data from tablet set C (Table 3), it was possible to conclude that there was a high probability that suspect tablets C-1 and C-2 were counterfeit and share a common tablet formulation. Spectra in Figure 5 show that the macro ATR spectra of suspect tablets C-1 and C-2 were not consistent with the macro ATR spectrum of authentic tablet C. This conclusion was based on spectral differences in the region around 1000 cm^{-1} and in the region between 3700 and 2800 cm^{-1}. Further, the macro ATR spectra of suspect tablets C-1 and C-2 were consistent with each other, and the same five compounds were detected using this technique (API-C, microcrystalline cellulose, inorganic carbonate, talc, and starch). Finally, the same six compounds were detected in each suspect sample using the micro ATR imaging technique (API-C, microcrystalline cellulose, inorganic carbonate, talc, starch, and an inorganic stearate).

dx.doi.org/10.1021/ac200957d |*Anal. Chem.* 2011, 83, 5972–5978

CONCLUSIONS

Counterfeit tablets have been analyzed using both macro ATR (nonimaging) and micro ATR imaging. The limitations of each technique are advantages of the other, which is why the two techniques complement each other so well. The macro ATR approach is a fast tool for counterfeit detection, but its use for determining tablet formulations is limited. On the other hand, the ATR imaging technique is slower and has limited use for detecting counterfeits but it is a more effective tool for characterizing tablet formulations. When it is of interest to both detect counterfeits and characterize counterfeit formulations for sourcing purposes, the most appropriate comprehensive approach involves using both techniques.

AUTHOR INFORMATION

Corresponding Author

*E-mail: adam.lanzarotta@fda.hhs.gov.

ACKNOWLEDGMENT

This work was first presented in Adam Lanzarotta's Ph.D. dissertation (Miami University, 2010).[52] The mentioning of specific products/instruments in this manuscript is for information purposes only and does not constitute an endorsement by either the Food and Drug Administration and/or the Forensic Chemistry Center. The authors would like to thank Fred Fricke and Dr. Duane Satzger from the FCC, Gloria Story from the Procter & Gamble Company, and all members of the MML group including Zachary Wenker.

REFERENCES

(1) U.S. Department of Health and Human Services. *Combating Counterfeit Drugs: A Report of the Food and Drug Administration*. http://counterfeiting.unicri.it/docs/FDA% 20combating%20ctf%20drugs.pdf (accessed April 2010).

(2) Witkowski, M.; Batson, J.; Crowe, J. Presented at the *Pittsburgh Conference*, Chicago, IL, March 2007; paper 640-5.

(3) Ranieri, N. Presented at the *Pittsburgh Conference*, Chicago, IL, March 2007; paper 640-6.

(4) Adar, F.; Witkowski, M.; Lee, E. Presented at the *Pittsburgh Conference*, Chicago, IL, March 2007; paper 640-7.

(5) Witkowski, M. R. *Am. Pharm. Rev.* **2005**, *56*, 58–62.

(6) Adar, F.; Lee, E.; Whitley, A.; Witkowski, M. *Raman Technology for Today's Spectroscopists* **2007**, 8–20.

(7) Lanzarotta, A.; Witkowski, M. R.; Sommer, A. J. Presented at the *Pittsburgh Conference*, Chicago, IL, March 2009; paper 2510-3.

(8) Bellamy, L. J. *The Infrared Spectra of Complex Molecules*, Richard Clay and Company, Ltd.: Bungay, Suffolk, Great Brittain, 1954; pp 253−260.

(9) Kalinkova, G. N.; Stoeva *Int. J. Pharm.* **1996**, *135*, 111–114.

(10) Pikal, M. J.; Lukes, A. L.; Lang, J. E. *J. Pharm. Sci.* **1977**, *66*, 1312–1316.

(11) Ahlneck, C.; Zografi, G. *lnt. J. Pharm.* **1990**, *62*, 87–95.

(12) Otsuka, M.; Kaneniwa, N. *Int. J. Pharm.* **1990**, *62*, 65–73.

(13) Kalinkova, G.; Ovcharova, G. *Pharmacia* **1994**, *6*, 24–26.

(14) Pinnamaneni, S.; Das, N. G.; Das, S. K. *Pharmazie* **2002**, *54*, 291–300.

(15) Chemburkar, S. R.; Bauer, J.; Deming, K.; Spiwek, H.; Patel, K.; Morris, J.; Henry, R.; Spanton, S.; Dziki, W.; Porter, W.; Quick, J.; Bauer, P.; Donaubauer, J.; Narayanan, B. A.; Soldani, M.; Riley, D.; McFarland, K. *J. Org. Process Res. Dev.* **2000**, *4*, 413–417.

(16) Huang, L.; Tong, W. *Adv. Drug Delivery Rev.* **2004**, *56*, 321–334.

(17) Lin, S. *J. Pharm. Sci.* **1988**, *77*, 229–232.

(18) Higuchi, T. *J. Pharm. Sci.* **1963**, *12*, 1145–1149.

(19) Patel, H.; Stalcup, A.; Dansereau, R.; Sakr, A. *Int. J. Pharm.* **2003**, *264*, 35–43.

(20) Nokhodchi, A.; Bolourtchian, N.; Farid, D. *Drug Dev. Ind. Pharm.* **1999**, *25*, 711–716.

(21) Edwards, I. R.; Aronson, J. K. *Lancet* **2000**, *356*, 1255–1259.

(22) Pawar, S.; Kumar, A. *Pediatric Drugs* **2002**, *6*, 371–379.

(23) Smith, J. M.; Dodd, T. R. P. *Adverse Drug React. Acute Poisoning Rev.* **1982**, *1*, 93–142.

(24) Weiner, M. *Adverse Reactions to Drug Formulation Agents: A Handbook of Excipients*; Marcel Dekker Inc.: New York, 1989; pp 89−120.

(25) Lyon, R. C.; Lester, D. S.; Lewis, E. N.; Lee, E.; Yu, L. X.; Jefferson, E. H.; Hussain, A. S. *AAPS Pharm. Sci. Tech.* **2002**, *3*, 1–15.

(26) Lee, E.; Huang, W. X.; Chen, P.; Lewis, E. N.; Vivilecchia, R. V. *Spectroscopy* **2006**, *21*, 24–32.

(27) Dubois, J.; Wolff, J.; Warrack, J. K.; Schoppelrei, J.; Lewis, E. N. *Spectroscopy* **2007**, *22*, 40–50.

(28) McCreery, R. L. *Raman Spectroscopy for Chemical Analysis*; John Wiley & Sons: New York, 2000.

(29) Grasselli, J. G.; Bulkin, B. J. *Analytical Raman Spectroscopy*; John Wiley & Sons: New York, 1991.

(30) Vankeirsbilck, T.; Vercauteren, A.; Baeyens, W.; Van der Weken, G.; Verpoort, F.; Vergote, G.; Remon, J. P. *TrAC, Trends Anal. Chem.* **2002**, *21*, 869–877.

(31) Bugay, D. E. *Adv. Drug Delivery Rev.* **2001**, *48*, 43–65.

(32) Huong, P. V. J. *Pharm. Biomed. Anal.* **1986**, *4*, 811–823.

(33) Bell, S. E. J.; Burns, D. T.; Dennis, A. C.; Matchett, L. J.; Speers, J. S. *Analyst* **2000**, *125*, 1811–1815.

(34) Pinzaru, S. C.; Pavel, I.; Leopold, N.; Kiefer, W. *J. Raman Spectrosc.* **2004**, *35*, 338–346.

(35) Ricci, C.; Eliasson, C.; Macleod, N. A.; Newton, P. N.; Matousek, P.; Kazarian, S. G. *Anal. Bioanal. Chem.* **2007**, *389*, 1525–1532.

(36) Chan, K. L. A.; Hammond, S. V.; Kazarian, S. G. *Anal. Chem.* **2003**, *75*, 2140–2146.

(37) van der Weerd, J.; Chan, K. L. A.; Kazarian, S. G. *Vib. Spectrosc.* **2004**, *35*, 9–13.

(38) van der Weerd, J.; Kazarian, S. G. *Appl. Spectrosc.* **2004**, *58*, 1413–1419.

(39) Elkhider, N.; Chan, K. L. A.; Kazarian, S. G. *J. Pharm. Sci.* **2006**, *96*, 351–360.

(40) Chan, K. L. A.; Kazarian, S. G. *Analyst.* **2006**, *131*, 126–131.

(41) Ricci, C.; Nyadong, L.; Fernandez, F. M.; Newton, P. N.; Kazarian, S. G. *Anal. Bioanal. Chem.* **2007**, *387*, 551–559.

(42) Lanzarotta, A.; Baumann, L.; Story, G. M.; Witkowski, M. R.; Khan, F.; Sommers, A.; Sommer, A. J. *Appl. Spectrosc.* **2009**, *63*, 979–991.

(43) Harrick, N. J. *Internal Reflection Spectroscopy*; Interscience Publishers: New York, 1967.

(44) *Modern Techniques in Applied Molecular Spectroscopy*; Mirabella, F. M., Ed.; John Wiley & Sons: New York, 1998.

(45) Lewis, L.; Sommer, A. J. *Appl. Spectrosc.* **1999**, *53*, 375–380.

(46) Lewis, L.; Sommer, A. J. *Appl. Spectrosc.* **2000**, *54*, 324–330.

(47) Patterson, B. M.; Havrilla, G. J. *Appl. Spectrosc.* **2006**, *60*, 1256–1266.

(48) Lanzarotta, A.; Gratz, S.; Brueggemeyer, T. W.; Witkowski, M. R. *Spectroscopy* **2011**, *26*, 34–41.

(49) Ellis, B.; Pyszora, H. *Nature* **1958**, *181*, 181–182.

(50) Dansereau, R.; Peck, G. E. *Drug Dev. Ind. Pharm.* **1987**, *13*, 975–999.

(51) Houck, M. M. *Trace Evidence Analysis More Cases in Mute Witnesses*; Elsevier Academic Press: Burlington, MA, 2004.

(52) Lanzarotta, A. Ph.D. Thesis, Miami University, Oxford, OH, May 2010. Available online http://etd.ohiolink.edu/view.cgi?acc_num=miami1272740376.

NOTE ADDED AFTER ASAP PUBLICATION

This paper was published on the Web on July 1, 2011, with an error in the caption of Figure 4. The corrected version was reposted on July 8, 2011.